Journal of Zhejiang University-SCIENCE B 2026 27(3):250-263
www.jzus.zju.edu.cn; www.springer.com/journal/11585
E-mail: jzus_b@zju.edu.cn

Research Article
https://doi.org/10.1631/jzus.B2400427

Check for updates

Integrative combination of gas–liquid-phase plasma mutagenesis and high-throughput screening to enhance eicosapentaenoic acid production by *Schizochytrium* sp.

Chao YU[1,2,3*], Jialin ZHU[4,5*], Jinyong WU[2], Xiangsong CHEN[1,2], Shuhuan LU[3], Xiangyu LI[3], Sa ZHAO[3], Weiwei ZHU[3], Min SHU[3], Mianbin WU[4,5✉], Jianming YAO[1,2✉]

[1]*University of Science and Technology of China, Hefei 230026, China*
[2]*Hefei Institutes of Physical Science, Chinese Academy of Sciences, Hefei 230031, China*
[3]*Cabio Biotech (Wuhan) Biotechnology Co., Ltd., Wuhan 430223, China*
[4]*Key Laboratory of Biomass Chemical Engineering of Ministry of Education, College of Chemical and Biological Engineering, Zhejiang University, Hangzhou 310030, China*
[5]*Ningbo Global Innovation Center, Zhejiang University, Ningbo 315100, China*

Abstract: Dietary consumption of eicosapentaenoic acid (EPA) offers diverse health benefits, such as the regulation of blood triglycerides and the prevention of cardiovascular diseases. EPA is naturally synthesized by *Schizochytrium* sp.; however, its low production level limits its potential for industrial application. The goal of this study was to increase EPA productivity in *Schizochytrium* sp. by gas–liquid-phase plasma (GLPP) mutagenesis combined with a high-throughput screening method. First, a diverse array of mutants was generated through GLPP mutagenesis. Next, the mutants with elevated EPA productivity were identified through near-infrared spectroscopy (NIRS). Notably, the M7-25 mutant demonstrated the highest and most consistent EPA production. After the culture medium was optimized, the EPA titer increased from 0.45 to 1.70 g/L. Finally, a cofermentation strategy using ammonia and glucose feeding was employed, and the EPA titer reached 2.08 g/L in a 7-L fermenter. This study reports the highest EPA titer achieved in *Schizochytrium* sp. via mutagenesis to date, highlighting its great market potential for industrial production.

Key words: Eicosapentaenoic acid (EPA); *Schizochytrium* sp.; Mutagenesis; High-throughput screening; Near-infrared spectroscopy (NIRS)

1 Introduction

Eicosapentaenoic acid (EPA) is an important functional food component that strongly supports human growth and development (Jia et al., 2022). Numerous studies have confirmed the effectiveness of EPA in preventing cardiovascular disease (Bhatt et al., 2019; Preston Mason, 2019; Khan et al., 2021), cancer (Liu YY et al., 2021; Yin et al., 2022), and depression (Bazinet et al., 2020; Peng et al., 2020); reducing inflammation (Calder, 2013; Lamon-Fava et al., 2021); and improving cellular antioxidant capacity (Xiao et al., 2022). Furthermore, recent research has shown that EPA may significantly reduce coronavirus disease symptoms (Doaei et al., 2021; Kosmopoulos et al., 2021). The demand for EPA has been growing rapidly. EPA is mainly found in oily deep-sea fish such as salmon, tuna, and mackerel. However, the current supply of EPA from aquaculture and fisheries meets only 30% of the global demand (Hamilton et al., 2020) due to factors such as increasing global population and stagnation of fishery production over the past five years caused by global warming (Auchterlonie and Bescoby, 2021). Thus, methods to sustainably manufacture EPA are desperately needed to eliminate shortages.

✉ Jianming YAO, jmy63@ipp.ac.cn
Mianbin WU, wumb@zju.edu.cn
* The two authors contributed equally to this work
Jianming YAO, https://orcid.org/0000-0001-6469-5380
Mianbin WU, https://orcid.org/0000-0001-6962-9702
Chao YU, https://orcid.org/0009-0002-6291-699X
Jialin ZHU, https://orcid.org/0009-0000-3313-2315

Received Aug. 19, 2024; Revision accepted Oct. 13, 2024; Crosschecked Nov. 22, 2025; Published online Dec. 22, 2025

To address the current shortage, researchers are searching for alternative sources of EPA, particularly from microorganisms. *Schizochytrium* sp. is considered an excellent candidate for EPA production because of its naturally high lipid content and its EPA synthesis pathway. *Schizochytrium* sp., belonging to the Thraustochytrids family, is a heterotrophic marine microalgal commonly found in seawater in Australia (Gupta et al., 2013), China (Ling et al., 2015), the Antarctic region (Shene et al., 2020), and other areas. Since the 1990s, *Schizochytrium* sp. has been utilized for commercial production of docosahexaenoic acid (DHA) (Ratledge and Hopkins, 2006). However, compared to the production of DHA, the production of EPA by Thraustochytrids strains is much less efficient. Jiang et al. (2004) isolated five Thraustochytrids strains and found that the ratio of EPA to total fatty acid (TFA) was no more than 1%. A strain isolated by Shene et al. (2020), Antarctic Thraustochytrids RT2316-7, exhibited an EPA/TFA ratio of 16.4% when cultured at 15 °C. However, the overall lipid content of this strain was extremely low.

To improve EPA productivity, Zeng et al. (2021) applied atmospheric and room-temperature plasma (ARTP) mutagenesis to *Schizochytrium* ATCC 20888, producing a mutant with an EPA titer of 0.48 g/L, which was 1.08-fold greater than that of the wild-type strain. Ou et al. (2023) also applied ARTP mutagenesis to *Schizochytrium* ATCC 20888, achieving an EPA titer of 1.86 g/L, with EPA accounting for 5.86% of the TFA. Similarly, ribosome engineering as a classic mutagenesis strategy has been successfully used to improve the neutral protease activity of *Bacillus amyloliquefaciens* (Zhu et al., 2025). Although the EPA productivity of *Schizochytrium* has improved, industrial application is still a distant possibility due to its low productivity and EPA content. The use of mutagenesis to improve EPA productivity in *Schizochytrium* has several technical limitations. The primary challenge involves the generation of mutants with highly diverse fatty acid (FA) profiles. Efficiently identifying mutants with high EPA productivity from a large pool of candidates is another obstacle. In response to these challenges, we employed a new physical mutagenesis technique known as gas–liquid-phase plasma (GLPP) mutagenesis. As depicted in Fig. 1, GLPP is generated from the discharge of O_2/air gas into the cell cultivation broth, which results in the generation of reactive nitrogen species (NO/HNO_2/HNO_3/ONOOH) and reactive oxygen species (OH·/H_2O_2/O_3) in the liquid phase (Morabit et al., 2021).

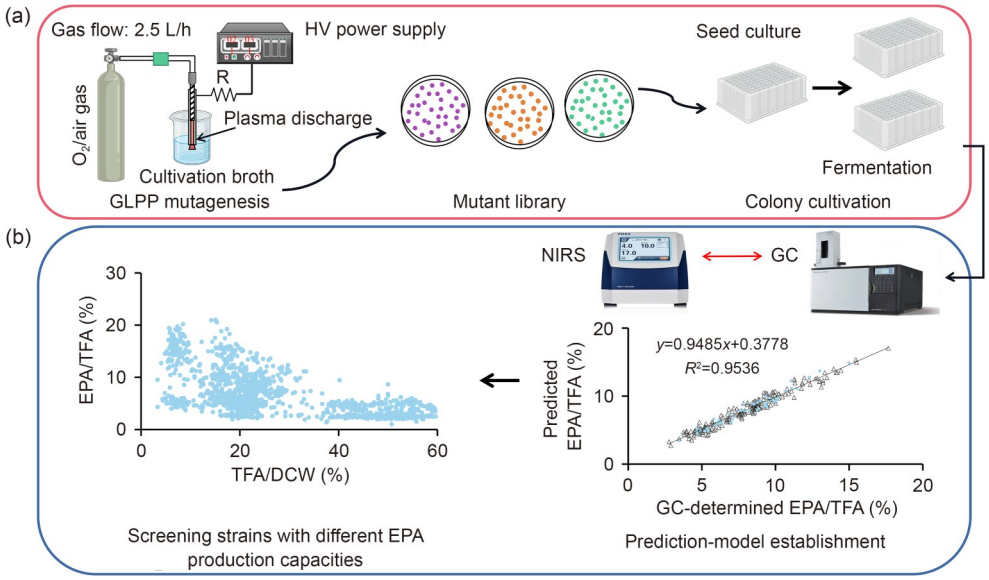

Fig. 1 Design of the gas–liquid-phase plasma (GLPP) mutagenesis and high-throughput screening platform for generating strains with different eicosapentaenoic acid (EPA) production capacities. (a) The liquid culture of *Schizochytrium* sp. was treated with GLPP to generate a mutant library. Single colonies were cultured in 24-well plates as seed-cultivation broth and then transferred to different 24-well plates for fermentation. (b) Samples of fermentation broth were scanned with near-infrared spectroscopy (NIRS) and analyzed with gas chromatography (GC), which generated enough data to establish a robust NIRS prediction model. This model was subsequently used to predict the EPA-production ability of the mutant strains. HV: high voltage; TFA: total fatty acid; DCW: dry cell weight.

These reactive species can inflict damage on cellular structures or genomes, potentially causing mutations or cell death. Consequently, GLPP is commonly employed to sterilize water contaminated with bacteria (Shen et al., 2019). However, by carefully modulating the discharge energy, GLPP can be employed to induce mutations in microorganisms. Regarding the second challenge, gas chromatography (GC), a traditional method for determining FA composition, is labor-intensive and time-consuming. In contrast, recent advances in near-infrared spectroscopy (NIRS) offer a swift and nondestructive alternative for determining the chemical composition of a compound or solution; this technique works by measuring the absorption of near-infrared radiation. Indeed, several studies have demonstrated that NIRS can be utilized to assess FA compositions (Yu et al., 2020; Reis et al., 2022; Tsegay et al., 2023). Because of the advantages of GLPP and NIRS, we combined these two powerful tools to establish a highly efficient platform for generating and detecting mutants with different levels of EPA productivity, as presented in Fig. 1.

In this study, we aimed to improve the production of EPA by *Schizochytrium* sp. through mutagenesis. First, we used GLPP to create a broad array of mutants in *Schizochytrium* sp. Then we developed an analytical method using NIRS technology to measure the ratio of TFA to dry cell weight (DCW) and determine the FA composition of the mutants. Genetic stability assessment was performed to confirm that the M7-25 mutant was stable for EPA production. Next, we optimized the concentrations of salt and phosphorus to increase the EPA titer. This step increased the concentration of TFA from 8.38 to 18.64 g/L and increased the EPA titer substantially from 1.15 to 1.58 g/L. Furthermore, when fermentation was scaled up to 7 L, the EPA titer of M7-25 reached 2.08 g/L, and the EPA/TFA ratio increased to 9.58%, representing a 1.77-fold and 3.05-fold increase, respectively, compared with the titer and ratio in the wild-type (WT) strain. We obtained a large number of mutant strains by GLPP mutagenesis, and then used high-throughput NIRS technology to identify mutant strains with high EPA production (Fig. 1). After performing medium and process optimization, we achieved the highest level of EPA production among known nongenetically manipulated *Schizochytrium* sp. strains, demonstrating that the strain has significant potential for large-scale industrial production.

2 Materials and methods

2.1 Strain, medium, and cultivation conditions

Schizochytrium sp. A-2 (CCTCC No.: M2012494) was used as the starting strain. The seed culture medium consisted of glucose (50 g/L), sodium glutamate (20 g/L), yeast extract (10 g/L), KH_2PO_4 (3 g/L), $MgSO_4$ (8 g/L), and NaCl (20 g/L). The fermentation medium consisted of glucose (100 g/L), sodium glutamate (20 g/L), yeast extract (15 g/L), and KH_2PO_4 (1.5 g/L) supplemented with either artificial sea salt or natural sea salt (NSS, East Sea of China). The artificial sea salt included $MgSO_4$ (3 g/L), Na_2SO_4 (25 g/L), $(NH_4)_2SO_4$ (5 g/L), KCl (1 g/L), $CaCl_2$ (0.15 g/L), and $NaHCO_3$ (0.2 g/L).

For high-throughput cultivation, the mutants were inoculated into 48-deep-well plates, with each well containing 1.5 mL of the seed culture medium. The plates were placed in a shaker at 28 °C with shaking at 230 r/min for 36 h. At the end of cultivation, the seed broth was transferred to another 48-deep-well plate, with each well containing 1.5 mL of fermentation medium. These plates were incubated again under the same conditions for 120 h.

For shake-flask fermentation, the mutants were cultured in seed culture medium for two generations, after which 2 mL of the seed medium was transferred to 250-mL shake flasks that were filled with 40 mL of fermentation medium. The fermentation experiments were carried out in a shaker set at 28 °C for 120 h with shaking at 230 r/min. The pH of the medium was not adjusted.

2.2 GLPP mutagenesis

The starting strain was cultivated in a 250-mL shake flask. Following incubation, the culture broth was centrifuged at 6000 r/min for 5 min, after which the cells were harvested and washed with 20 mL of sterile water. The washed cells were resuspended in a sterile 9 g/L NaCl solution, with the volume matching the original culture volume, resulting in an optical density at 600 nm (OD_{600}) of approximately 20 min. The cell suspension was treated with GLPP for 5, 10, 15, or 20 min. The discharge power of the GLPP was set at 12.7 V, and the discharge peak current was set at either 1.5 or 2.0 A. Subsequently, the sample was diluted, spread on solid plates, and incubated at 28 °C for 48 h. The number of colonies was recorded, and the lethality of the cells was calculated according to the following formula:

$$L = \frac{n_{\text{con}} - n_{\text{GLPP}}}{n_{\text{con}}} \times 100\%,$$

where L is lethality, n_{con} is colony number of control, and n_{GLPP} is colony number with GLPP.

2.3 Quantification of DCW and TFA, and FA composition

DCW was quantified as follows: 1.0 mL of fermentation broth was harvested, and the cells were collected by centrifugation (6000 r/min, 3 min), followed by lyophilization. The DCW (g/L) was calculated as follows:

$$\text{DCW} = W/V,$$

where W is freeze-dried cell weight and V is sample volume.

For TFA extraction and fatty acid methyl ester (FAME) analyses, we followed the method described by Yue et al. (2019). The EPA/DCW (r_{ED}) was calculated by the internal standard method (Golay and Moulin, 2016). The EPA/TFA (r_{ET}) ratio was the proportion of the peak area of EPA to the total peak area. The TFA/DCW (r_{TD}) ratio was calculated using the following formula:

$$r_{\text{TD}} = r_{\text{ED}}/r_{\text{ET}}.$$

2.4 Prediction-model development by NIRS

The FOSS NIR spectrophotometer (NIRS™ DA1650, Hilleroed, Denmark) uses diffuse reflection to measure the transmission and reflectance spectra of a sample over a wavelength range of 570–1880 nm. A total of 2 mL culture broth was centrifuged at 6000 r/min for 5 min, after which the cells were harvested and washed with 10 mL of tap water. The washed cells were then dispersed in 2 mL of tap water. The cell suspension was scanned five times to form an average NIR spectrum, which was then transformed into log(1/R) format, where R is the reflectance. We developed prediction models to quantify the TFA/DCW as well as the proportions of palmitic acid (PA), arachidonic acid (ARA), EPA, docosapentaenoic acid (DPA), and DHA to TFA. We used the modified partial least squares regression method and implemented it in WinISI III software (InfraSoft International, LLC, FOSS, PA, USA). The data quality assessment was evaluated using the root mean square error of cross-validation for each individual dataset.

2.5 Evaluation of mutants' genetic stability

The candidate mutants were cultivated in seed medium for seven successive passages. Each cultivation of the passage represented one generation, and the cultivation of each passage was inoculated into the fermentation medium and cultivated for 5 d. Then, the ratios of EPA/TFA and TFA/DCW were measured and compared with the ratios from the first generation. The mutant with the most stable genetic performance was used for further experiments.

2.6 Medium optimization and fed-batch fermentation

2.6.1 Shake-flask fermentation to optimize the medium

We used biological triplicates to analyze the DCW, FA composition, and TFA/DCW ratio. The medium optimization was performed as follows. (1) Salinity experiments: artificial sea salt and NSS were both tested at concentrations of 15, 25, 35, and 45 g/L, and the other components of the medium included 100 g/L glucose, 20 g/L sodium glutamate, 7.5 g/L yeast extract, and 1.5 g/L KH_2PO_4. (2) Phosphorus experiment: KH_2PO_4 concentrations were tested at concentrations of 0.1, 0.5, 1.5, and 3.5 g/L, and the other components of the medium were 25 g/L NSS, 100 g/L glucose, 20 g/L sodium glutamate, and 7.5 g/L yeast extract.

2.6.2 Fed-batch fermentation in a 7-L fermenter

The fed-batch fermentation was conducted using 7-L fermenters (Shanghai Baotech Engineering Co., Ltd., China). Three different fermentation batches were performed using: (1) WT strain, (2) M7-25 mutant strain, and (3) M7-25 mutant strain which was fed 25% (mass fraction) $NH_3 \cdot H_2O$ for 10–48 h. The seed culture was transferred to 4 L of fermentation medium with an inoculation ratio of 5% (volume ratio). The fermentation medium components were 25 g/L NSS, 100 g/L glucose, 20 g/L sodium glutamate, 7.5 g/L yeast extract, and 0.5 g/L KH_2PO_4. The fermentation temperature was set at 28 °C, and the pH was maintained at 7.6 by adding citrate acid. The dissolved oxygen was maintained at no lower than 20% (volume fraction) for 0–48 h and no higher than 10% for 48–144 h by adjusting the air-flow rate and agitation speed. The residual glucose concentration in the fermentation broth was maintained between 10 and 30 g/L by feeding a 600 g/L glucose solution. Fermentation broth was sampled every 12 h to analyze the DCW, TFA/DCW, and FA/TFA.

In addition, we performed pH experiments under the same fermentation conditions, in which the pH was maintained at 7.6 using various acid-base combinations: (1) citric acid+ammonia solution, (2) citric acid+sodium hydroxide, and (3) ammonium sulfate+sodium hydroxide.

2.7 Statistical analysis

The results are presented as mean±standard deviation (SD). Statistical significance between mean values was determined using Duncan's test.

3 Results and discussion

3.1 GLPP mutagenesis of *Schizochytrium* sp.

Schizochytrium sp. is the most commonly used strain for commercial production of DHA, and it could synthesize small amounts of EPA (Gupta et al., 2013; Shene et al., 2020). In this study, we employed the GLPP mutagenesis method to produce mutant strains of *Schizochytrium* sp. and obtain strains with high EPA productivity for future industrial application.

As shown in Fig. 2a, the lethality rate of cells increased rapidly at 5 min of exposure to GLPP at two different discharge peak currents. When the exposure time was increased, the lethality rate showed a diminishing trend in its rate of increase, which was consistent with the results of ARTP mutagenesis (Wei et al., 2023). After a 20-min exposure, the maximal lethality of the cells reached 82.4% and 98.1% at discharge peak currents of 1.5 and 2.5 A, respectively (P<0.05). These results indicated that compared to a lower current, a higher discharge peak current led to a higher lethality rate. To achieve a lethality rate of 90% (Liu L et al., 2021), we selected the condition of optimal discharge peak current of 2.5 A and an exposure period of 15 min to achieve a lethality rate of approximately 93.5%. The FA composition varied broadly in the resulting mutants compared with the WT strain, with EPA/TFA ranging from −38.44% to 68.50% and ARA/TFA ranging from −41.23% to 46.69% (Fig. 2b); in contrast, the variability for DHA/TFA and DPA/TFA was mainly in the range of −20% to 20% (Fig. 2c). The relative variation in PA/TFA ranged from −72.38% to 39.35% (Fig. 2d). The substantial range in EPA/TFA and ARA/TFA, along with the relative stability in DHA/TFA and DPA/TFA, reflects the high efficacy and randomness of GLPP in the induction of relevant mutations. Similar results were reported in recent studies that used ARTP

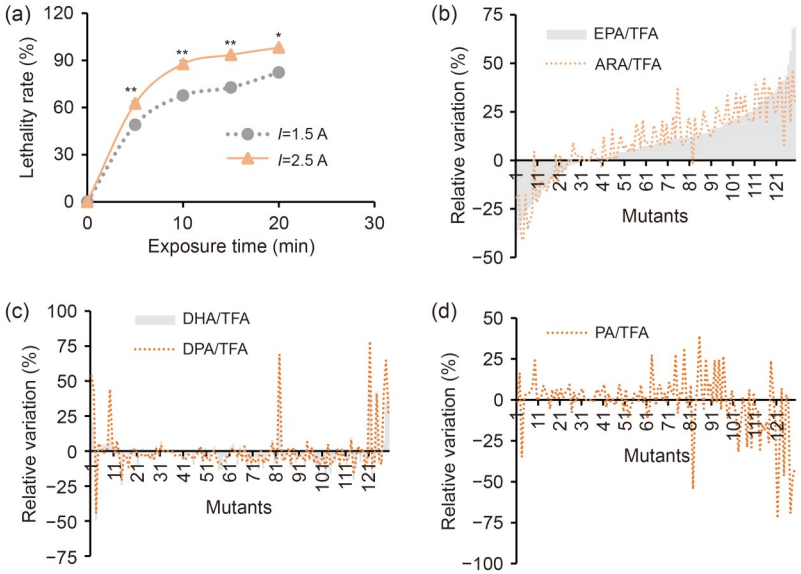

Fig. 2 Effects of gas–liquid-phase plasma (GLPP) on lethality rate and fatty acid composition in *Schizochytrium* sp. mutants. (a) Effects of different energy levels (I=1.5 A and I=2.5 A) and exposure time (5, 10, 15, and 20 min) of GLPP mutagenesis on the lethality rate of *Schizochytrium* sp. The data were collected from three independent experiments. Error bars represent the standard deviation. Significant differences between the I=1.5 A and I=2.5 A groups are indicated by asterisks (* P<0.05, ** P<0.01). (b–d) The relative variations in the proportions of eicosapentaenoic acid (EPA), arachidonic acid (ARA), docosahexaenoic acid (DHA), docosapentaenoic acid (DPA), and palmitic acid (PA) to total fatty acid (TFA) in the GLPP-induced mutants compared with the wild-type (WT) strain.

mutagenesis technology in *Schizochytrium*. For example, Wei et al. (2023) reported a 108% increase in the EPA titer, Ou et al. (2023) reported a more substantial increase (5.64-fold) in the EPA titer, and Wang et al. (2021) documented a 51% increase in DHA/TFA. These findings showed that ARTP mutagenesis can effectively enhance the biosynthesis of omega-3 fatty acids. In contrast, our study with GLPP mutagenesis revealed a unique trend in which EPA/TFA and ARA/TFA varied substantially, which also showed that GLPP mutagenesis with a discharge peak current of 2.5 A and an exposure period of 15 min was effective in the induction of mutations that can lead to improved EPA production in *Schizochytrium* sp.

3.2 High-throughput analysis of FA composition by NIRS

Traditional methods for screening mutants can be inefficient and cost-prohibitive (Zeng et al., 2020). Owing to the substantial number of mutants generated by GLPP mutagenesis, we considered it imperative to develop an efficient screening method that could swiftly and accurately identify strains with highly efficient EPA biosynthesis. Here, we used 194 samples for NIRS calibration, employing a modified partial least square regression methodology within WinSIS III to develop prediction models. The NIRS curves displayed a similar trend with abundant absorption in the 1300–1600 nm region, and each sample differed in terms of absorption in this region, which formed the basis for calculating and establishing the NIRS model (Fig. S1).

The key parameters for modeling the FA composition and TFA/DCW ratio are summarized in Table 1. The results suggest that the NIRS models are satisfactory for predicting TFA/DCW, EPA/TFA, and DHA/TFA, showing the best performance for TFA/DCW. Notably, our coefficient of determination (R^2) values were greater than those reported by Reis et al. (2022) (0.89) and Yu et al. (2020) (0.90). The improved fit of our model may be due to the removal of impurities from the fermentation broth by washing the cells with tap water, which improved modeling accuracy.

Table 1 Coefficient of determination and SECV of the calibration set for TFA/DCW, EPA/TFA, and DHA/TFA using NIRS

Parameter	Coefficient of determination (R^2)	SECV
TFA/DCW	0.963	1.555
EPA/TFA	0.947	0.935
DHA/TFA	0.901	1.948

SECV: standard error of cross-validation; TFA: total fatty acid; DCW: dry cell weight; EPA: eicosapentaenoic acid; DHA: docosahexaenoic acid; NIRS: near-infrared spectroscopy.

While the high R^2 value indicates that our model fits the training data well, it was also crucial to evaluate its predictive accuracy. To assess the model's accuracy, we selected a set of 48 mutant samples for use as an external validation set. A comparison between the NIRS predictions and reference values for TFA/DCW, EPA/TFA, and DHA/TFA is shown in Fig. 3. The biases between the prediction and reference values for TFA/DCW (Fig. 3a) and EPA/TFA (Fig. 3b) were generally less than 10%; only approximately 8.3% of the samples showed a bias exceeding 10% for EPA/TFA, and none of these biases surpassed 15%. Both the prediction and reference data biases were under 10% for DHA/TFA (Fig. 3c). Notably, the samples used for external validation were not part of the model development, ensuring an unbiased evaluation of model performance. Validating a model via random samples from one-third of the data is a critical step for assessing robustness (Yu et al., 2020). Our model validation tests revealed that NIRS can predict the FA composition of *Schizochytrium* reliably and accurately, which is consistent with previous studies showing that NIRS can be used to predict the FA composition of fish oil (Karunathilaka et al., 2019), pig fat (González-Martín et al., 2021), and milk-thistle whole seeds (Koláčková et al., 2015). In particular, our study showed that NIRS could accurately predict FA composition and, notably, enhance detection efficiency, offering a time-efficient alternative to GC detection. While 9.58 h was needed for GC analysis of a single sample, NIRS analysis was completed in 2 min (Table S1). NIRS proved effective, but Raman spectroscopy might also serve as an alternative for this application. Raman spectroscopy provides molecular vibration information, enabling rapid identification and quantification of metabolic products. Previous studies have demonstrated its potential in monitoring fermentation processes (Wang et al., 2014), quantifying lipids in microalgae with high accuracy compared to GC measurements (Lee et al., 2013), and predicting the FA composition of vegetable oils (Dong et al., 2013). While both NIRS and Raman spectroscopy are effective for rapid FA detection, our study focused on the application of NIRS. However, the throughput of the NIRS

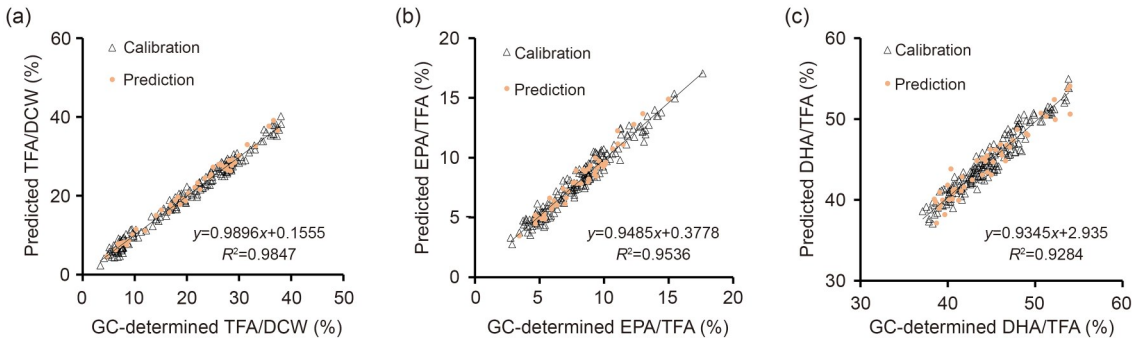

Fig. 3 Near-infrared spectroscopy (NIRS) prediction models for TFA/DCW (a), EPA/TFA (b), and DHA/TFA (c). The black triangles represent the calibration model, the yellow circles represent the test data. The data were collected from three independent experiments. TFA: total fatty acid; DCW: dry cell weight; EPA: eicosapentaenoic acid; DHA: docosahexaenoic acid; GC: gas chromatography.

apparatus is limited by its reliance on manual sample changeovers. Thus, automated sample changeover capabilities should be developed to further improve detection efficiency. Despite the limitations imposed by manual sample handling, NIRS significantly enhances detection efficiency and reduces costs, making it a valuable tool for analyzing and predicting the composition of FAs.

3.3 Identifying mutants with high FA and EPA production

After GLPP mutagenesis, we selected more than 3000 mutants, cultured them in 48-well plates, and then analyzed them with the NIRS models developed earlier. The predicted EPA/TFA and TFA/DCW values of the mutants are shown in Fig. 4a. The EPA/TFA ratio in 1469 mutants ranged from 2% to 21% with more than 53% of the mutants presenting higher levels of EPA/TFA than the WT strain, indicating that GLPP induces beneficial genetic mutations with higher efficacy. Similarly, the TFA/DCW ranged from 3.4% to 63.3%, and more than 30% of the mutants presented greater TFA/DCW than the WT strain.

We calculated the EPA titer, which indicates the efficiency of EPA production by multiplying EPA/TFA, TFA/DCW, and DCW. As shown in Fig. 4b, the highest EPA titer achieved in a mutant M108 was 1.65 g/L, which was 3.24-fold greater than that of the WT strain. Concurrently, the EPA/TFA and TFA/DCW ratios were 8.67% and 50.01%, respectively. Another mutant exhibited a similar EPA titer of 1.47 g/L, but with markedly different EPA/TFA and TFA/DCW ratios (15.69% for EPA/TFA and 16.80% for TFA/DCW). These results indicated that the mutants could be divided into two distinct groups: those with higher TFA/DCW values and lower EPA/TFA values, and those with lower TFA/DCW values and higher EPA/TFA values. In a study conducted by Ou et al. (2023), the optimal mutant obtained from ARTP exhibited an EPA/TFA ratio of 5.86% and a TFA/DCW ratio of 59.20%. Compared to ARTP, the use of GLPP led to a more significant variation in EPA/TFA. This difference may be attributable to the distinct mechanisms of the two types of mutagenesis. Although GLPP achieves a lethality rate of 93.5% in 15 min while ARTP reaches the same level in less than 1 min (Ou et al., 2023; Wei et al., 2023), GLPP can generate mutants with more diverse FA compositions; therefore, GLPP effectively increases genetic diversity. Based on these results, GLPP mutagenesis seems to be a valuable tool for enhancing the genetic diversity of microorganisms, potentially leading to the generation and isolation of mutants with new desirable properties.

We further evaluated the 48 mutants whose EPA/TFA ratios exceeded 15% via shake-flask fermentation. Among these 48 mutants, only six maintained the same EPA/TFA levels as the initially obtained mutants (Fig. 4c), and some mutants even presented lower EPA/TFA ratios (4.23%) than the WT strain. Therefore, most of the mutants were not stable. One explanation for this observation is that the DNA damage caused by the mutation triggered a DNA repair response, leading to elimination of the mutation and restoration of WT genetic sequences (Rosenberg, 2013; Chatterjee and Walker, 2017). This observation suggests that achieving stable and consistently high levels of EPA production could be a challenge, even though initial efforts to increase EPA/TFA through mutagenesis have shown promise. Nonetheless, we successfully identified three

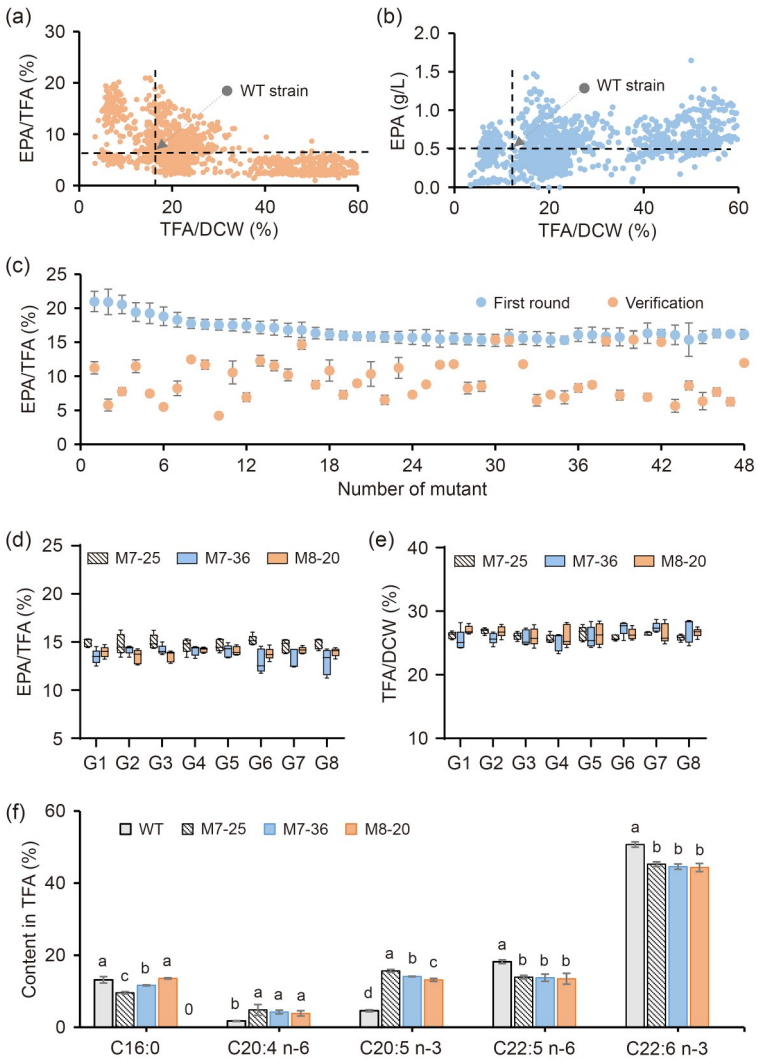

Fig. 4 High-throughput screening of *Schizochytrium* sp. mutants with highly efficient EPA production. (a) EPA/TFA and TFA/DCW of all the mutants cultured in 48-deep-well plates by near-infrared spectroscopy (NIRS) prediction. (b) EPA titer and TFA/DCW of all the mutants cultured in 48-deep-well plates. (c) Verification of EPA/TFA levels in the mutants grown through shake-flask cultivation. (d, e) Stability test of EPA/TFA (d) and TFA/DCW (e) of the mutants M7-25, M7-36, and M8-20 grown across eight generations (G1–G8) through shake-flask cultivation. (f) Main fatty-acid composition of the wild-type (WT) strain and the mutants M7-25, M7-36, and M8-20. C16:0, palmitic acid; C20:4 n-6, ARA; C20:5 n-3, EPA; C22:5 n-6, DPA; C22:6 n-3, DHA. The figures display average results obtained from at least three independent experiments, with error bars representing the standard deviation. Different lowercase letters indicate significant differences among each group based on Duncan's test (P<0.05). EPA: eicosapentaenoic acid; TFA: total fatty acid; DCW: dry cell weight; ARA: arachidonic acid; DPA: docosapentaenoic acid; DHA: docosahexaenoic acid.

mutants that presented persistently high levels of EPA/TFA.

Stability tests are crucial for ensuring that genetic mutations are maintained under normal production conditions. No significant differences (P>0.05) in the EPA/TFA (Fig. 4d) or TFA/DCW (Fig. 4e) ratio were found across eight passages in the three mutant strains: M7-25, M7-36, and M8-20. The average EPA/TFA ratios in these strains over eight passages were 14.83%, 13.65%, and 13.89%, respectively, and the TFA/DCW ratios were 26.17%, 26.24%, and 26.48%, respectively. These results suggest that the three mutants maintained stably across eight passages, indicating consistent genetic expression and metabolic performance. As shown in Fig. 4f, the EPA/TFA ratios of mutants M7-25, M7-36, and M8-20 were 2.42-, 2.08-, and 1.87-fold greater than those of the WT strain, respectively (P<0.05). Considering the degree of unsaturation, DHA and DPA

were the most abundant unsaturated FA, whereas C16:0 was the main saturated FA. M7-25 was selected for further analysis by its high EPA/TFA (15.65%) and ARA/TFA (4.8%) ratios, as compared to other EPA-producing strains (Ou et al., 2023).

We also identified a strong positive linear correlation with R^2=0.860 between EPA and ARA (Fig. S2), which has not been previously reported. According to a study conducted by Yue et al. (2019), ARA, EPA, DHA, and DPA shared a pool of acetyl-CoA and malonyl-CoA as precursors, which may explain the observed decreases in DHA/TFA and DPA/TFA with the increase in EPA/TFA. Although *Schizochytrium* sp. is known to synthesize DHA and n-6 DPA via the polyketide synthase (PKS) pathway, the EPA synthesis pathway involved remains elusive (Du et al., 2021). Nonetheless, the M7-25 mutant, which can synthesize high levels of EPA and ARA, may serve as a valuable resource for elucidating the EPA synthesis pathway. In conclusion, we identified a mutant (M7-25) with higher EPA/TFA and TFA/DCW levels than those of the WT strain, making it a suitable candidate for further optimization experiments.

3.4 Medium optimization to increase TFA and EPA production

Schizochytrium spp. are typically found in coastal waters; consequently, salinity is a critical factor for their FA synthesis (Sun et al., 2018a). We investigated the influence of different concentrations of artificial sea salt and NSS on EPA production. As shown in Fig. 5a, the EPA/TFA ratio increased from 9.60% to 13.76% as the artificial sea salt concentration increased from 15 to 25 g/L, but decreased to 9.65% at 45 g/L (P<0.05). Similarly, the TFA/DCW ratio decreased from 24.00% to 13.60% as the artificial sea salt concentration increased from 15 to 45 g/L (Fig. 5b). In the NSS group, the highest EPA/TFA ratio was 9.50% with an NSS concentration of 15 g/L, but decreased to 2.88% with an NSS concentration of 45 g/L (Fig. 5a). Although the EPA/TFA ratio was lower in the NSS group, the TFA and TFA/DCW ratio were significantly greater than those in the artificial sea salt group (P<0.05). The highest TFA concentration achieved in the NSS group was 15.29 g/L, which was 69.3% greater than the highest TFA concentration attained in the artificial sea salt group (Fig. 5b). Studies have indicated that

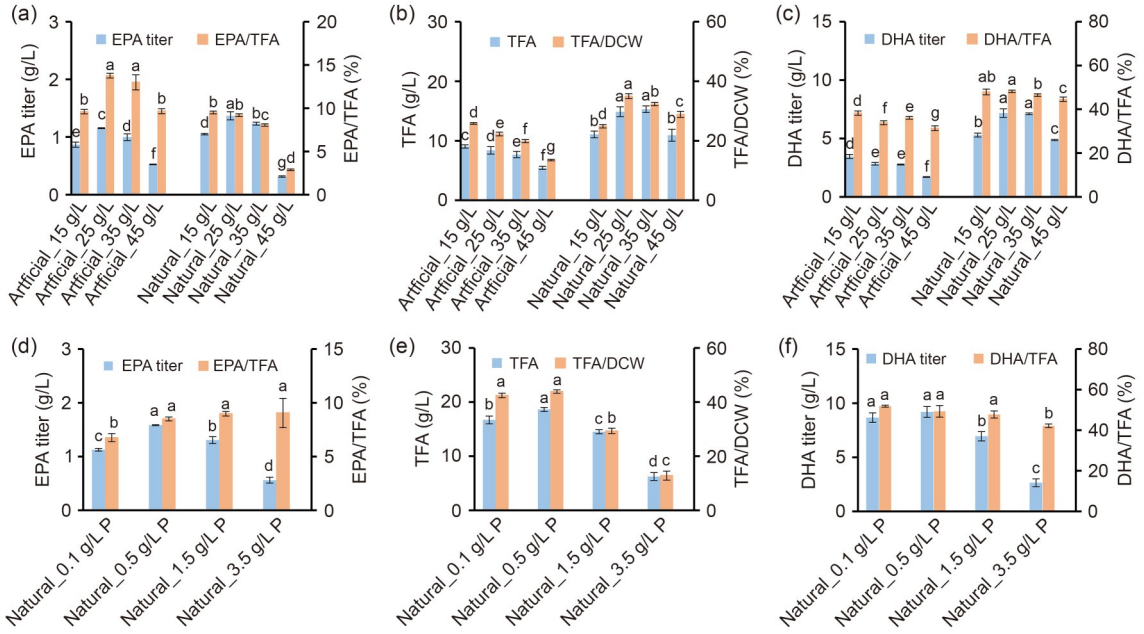

Fig. 5 Systematic evaluation of the impact of salt and phosphorus on FA biosynthesis in *Schizochytrium* sp. (a–c) Effects of different concentrations of artificial sea salt and natural sea salt (NSS) on the EPA titer and EPA/TFA (a), TFA and TFA/DCW (b), and DHA titer and DHA/TFA (c). (d–f) Effects of different concentrations of phosphorus (P) on the EPA titer and EPA/TFA (d), TFA and TFA/DCW (e), and DHA titer and DHA/TFA (f) with 25 g/L NSS. The figures show the average results obtained from three independent experiments, with error bars representing the standard deviation. Different lowercase letters indicate significant differences among groups according to Duncan's test (P<0.05). EPA: eicosapentaenoic acid; TFA: total fatty acid; DCW: dry cell weight; DHA: docosahexaenoic acid; P: KH_2PO_4.

moderate salinity stress can increase lipid accumulation in *Schizochytrium* sp., whereas extreme salinity may inhibit lipid production (Sun et al., 2018b; Chen et al., 2023). Therefore, identifying the most appropriate salinity is essential for the industrial production of lipids from *Schizochytrium* sp. The highest EPA titers attained in the artificial and natural salt groups were 1.15 g/L and 1.37 g/L, respectively; both had a salinity of 25 g/L, but the EPA titer significantly decreased when the salinity increased to 45 g/L (P<0.05) (Fig. 5a).

Considering the importance of lipid extraction efficiency for algae oil production, we applied two mutant strains (M7-25 and M108) in a 7-L-scale fermentation to obtain substantial biomass. M7-25 exhibits lower TFA/DCW but a higher EPA/TFA ratio, while M108, a mutant derived from GLPP mutagenesis, has opposite results (Fig. S3). Lipids were extracted after fermentation, and the oil is shown in Fig. S4. As shown in Table 2, batch 2#, with the lowest TFA/DCW ratio (21.78%), presented the lowest TFA extraction yield of 20.41%. In contrast, batch 4#, with the highest TFA/DCW ratio (52.00%), demonstrated a markedly greater extraction TFA yield of 85.86%. This suggested that the TFA/DCW ratio is associated with TFA extraction efficiency. One possible explanation is that in low-lipid cells, lipids are more tightly bound within cell structures rather than being freely dispersed, making them less accessible to solvents. Additionally, higher proportions of non-lipid materials can hinder solvent penetration and lipid solubilization. Therefore, a higher TFA/DCW ratio enhances solvent access to lipids, resulting in increased extraction efficiency and yield. According to the study by Derwenskus et al. (2020), the most expensive stage of the production of EPA from *Phaeodactylum tricornutum* is the extraction and purification process. Therefore, culture with NSS is more advantageous than with artificial sea salt. Chen et al. (2023) also demonstrated that NSS is suitable for producing oil from *Schizochytrium* sp. Fig. 5c shows that both the DHA/TFA ratio and DHA titer were significantly greater in the NSS group than in the artificial sea salt group (P< 0.05). This result further verified the idea that NSS is more suitable for promoting FA production from *Schizochytrium* sp.

Phosphorus is also essential for algae because it plays a crucial role in synthesizing phospholipids and triacylglycerols (Ren et al., 2013). As shown in Fig. 5d, increasing the KH_2PO_4 concentration from 0.1 to 1.5 g/L led to an increase of 30.8% in the EPA/TFA ratio (P< 0.05). The highest EPA titer of 1.70 g/L was attained at 0.5 g/L KH_2PO_4. Fig. 5e shows that increasing the KH_2PO_4 concentration from 0.5 to 1.5 g/L resulted in a notable decrease in TFA/DCW and TFA (to 29.35% and 14.52 g/L, respectively), which further decreased to 12.83% and 6.25 g/L, respectively, as the KH_2PO_4 concentration increased to 3.5 g/L (P<0.05). Ren et al. (2013) reported that KH_2PO_4 concentrations between 0.1 and 0.5 g/L significantly increased TFA production, whereas higher concentrations decreased TFA production and the TFA/DCW ratio in *Schizochytrium* sp. These findings suggest that KH_2PO_4 profoundly influences TFA synthesis in *Schizochytrium* sp. Fig. 5f shows that the DHA titer followed the same trend as that of TFA production; the DHA/TFA ratio significantly decreased at 3.5 g/L KH_2PO_4 (P<0.05). Therefore, 0.5 g/L KH_2PO_4 was optimal for both the EPA and DHA concentrations in NSS. In summary, we found that 25–35 g/L NSS and appropriate phosphate limitation are important for EPA and TFA production.

3.5 Fed-batch fermentation

The potential of mutant strain M7-25 for EPA production was validated in 7-L fermenters. Fig. 6a shows that the DCW of M7-25 did not significantly differ from that of the WT strain before 96 h. However, the amount of TFA produced by M7-25 reached a maximum of 17.01 g/L at 72 h, which was 35.8% greater than the maximum amount produced by the WT strain. This increase was mainly attributable to the higher TFA/DCW ratio in M7-25 than in the WT. Feeding

Table 2 Extraction efficiency based on the fermentation of mutant strains

Batch	Strain	TFA (g/L)	TFA/DCW (%)	Theoretical TFA (g)	Extracted TFA (g)	Extraction efficiency (%)
1#	M7-25	10.81	24.02	97.3	25.8	26.52
2#	M7-25	10.89	21.78	98.0	20.0	20.41
3#	M7-25	11.66	25.91	186.6	42.0	22.51
4#	M108	28.60	52.00	257.4	221.0	85.86

TFA: total fatty acid; DCW: dry cell weight.

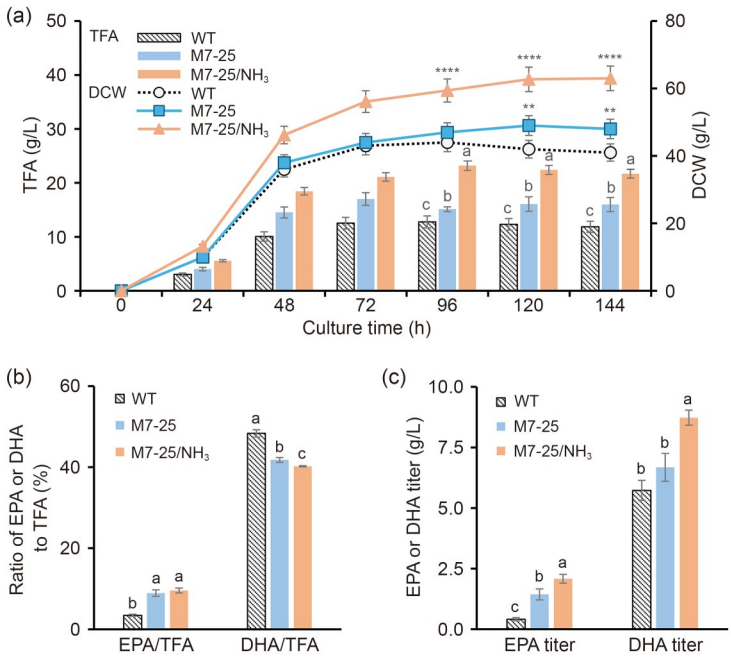

Fig. 6 Fed-batch fermentation of *Schizochytrium* sp. conducted in 7-L fermenters with different strains and fermentation strategies: wild type (WT) (glucose feeding); M7-25 (glucose feeding); and M7-25/NH_3 (glucose and $NH_3 \cdot H_2O$ feeding). (a) Time courses of dry cell weight (DCW) and total fatty acid (TFA) in fed-batch culture. Significant differences among groups are indicated by asterisks (** P<0.01, **** P<0.0001 vs. WT). (b) Ratios of eicosapentaenoic acid (EPA) to TFA (EPA/TFA) and docosahexaenoic acid (DHA) to TFA (DHA/TFA) in *Schizochytrium* sp. at 144 h in fed-batch culture. (c) EPA and DHA titers in *Schizochytrium* sp. at 144 h in fed-batch culture. A concentration of 600 g/L glucose solution was added to the fermentation broth as needed to maintain a glucose concentration between 10 and 20 g/L. The air flow rate and agitation speed were adjusted to maintain dissolved oxygen levels above 20% during the initial 0–48 h and at 10% for the remaining 48–144 h. The figures show the average results obtained from at least three independent experiments, with error bars indicating the standard deviation. Different lowercase letters indicate significant differences among groups according to Duncan's test (P<0.05).

with ammonia water (M7-25/NH_3 group) led to a notable improvement in both DCW and TFA production. The DCW in the M7-25/NH_3 group reached 63.0 g/L, which was 53.7% greater than that in the WT group (P< 0.0001). The amount of TFA in the M7-25/NH_3 group increased to 23.19 g/L, representing a 53.4% increase compared with that in the M7-25 group and an 81.6% increase compared with that in the WT group at 96 h. The results shown in Fig. S5 demonstrate that the combination of $(NH_4)_2SO_4$ and NaOH also supported cell growth and TFA production. In contrast, using a combination of NaOH and citrate acid to adjust pH resulted in lower DCW and TFA, suggesting that the absence of NH_4^+ limits both cell growth and lipid synthesis. The notable increase in TFA and DCW with the addition of ammonia indicates that nitrogen availability plays a crucial role in promoting cell growth and lipid synthesis. This finding aligns with those of a study by Yin et al. (2019), which showed that ammonia significantly promotes biomass and lipid accumulation in *Schizochytrium* sp.

Fig. 6b shows that the EPA/TFA ratio in the M7-25/NH_3 group reached 9.58%, which was 1.77-fold greater than the ratio in the WT group at the end of fermentation (P<0.05). Notably, a comparison between the M7-25 and M7-25/NH_3 groups revealed that the EPA/TFA ratios were not significantly different, suggesting that ammonia supplementation did not affect the EPA/TFA ratio (P>0.05). Additionally, the DHA/TFA level in the M7-25/NH_3 group was comparable to that in the M7-25 group and 16.79% lower than that in the WT group. The noticeable reduction in the DHA/TFA level compared to that in the WT group highlights the effects of the induced mutations on FA synthesis in *Schizochytrium* sp. Finally, the EPA titer in the M7-25/NH_3 group reached 2.08 g/L, which was 4.05-fold greater than that in the WT group (P<0.05). This is the greatest increase among the strains of *Schizochytrium* sp. obtained by mutagenesis technology (Table 3). The DHA concentration also increased by 52.4%, from 5.7 to 8.7 g/L (Fig. 6c), indicating that ammonia

Table 3 Ability of *Schizochytrium* sp. to produce EPA

Strain	Strategy	EPA/TFA (%)	EPA titer (mg/L)	Reference
Schizochytrium ATCC 20888	ARTP	3.47	480	Zeng et al., 2021
Schizochytrium ATCC 20888	ARTP	5.87	1860	Ou et al., 2023
Schizochytrium sp. CABIO-A-2-IV	GLPP	9.58	2080	This study

EPA: eicosapentaenoic acid; ARTP: atmospheric and room-temperature plasma mutagenesis; GLPP: gas–liquid-phase plasma mutagenesis; TFA: total fatty acid.

supplementation with the M7-25 mutant substantially increased production of EPA and DHA. However, despite an impressive omega-3 production of 10.78 g/L, there remains a substantial gap compared to the industrial DHA production of 46.4 g/L (Chen et al., 2023), which poses a major bottleneck for industrialization. In addition to this, research on oil separation and purification processes is still needed to finalize the product. We speculate that the EPA production of M7-25 could be further improved by continued GLPP mutagenesis and fermentation optimization to facilitate large-scale industrial production of EPA in *Schizochytrium* sp. Furthermore, the combined GLPP and NIRS platform is not limited to optimizing EPA production in *Schizochytrium* sp.; it can also be applied to improve the efficiency of other microbial products. GLPP induces mutations throughout the genome, creating a diverse pool of mutants with potentially beneficial traits, while NIRS provides a non-destructive and rapid method to quantify desired products, enabling swift identification of high-performing strains. Therefore, the strains, whether genetically modified or not, reach the limits of their production capacity; this methodology offers an alternative route to discover unforeseen enhancements in production.

4 Conclusions

In conclusion, we developed an innovative strategy to increase EPA production in *Schizochytrium* sp. involving GLPP mutagenesis followed by NIRS screening, which enables the identification of high-yield strains from a 1469-mutant library in just one week. This method is much more efficient than traditional mutagenesis strategies. Compared with the WT strain, the M7-25 mutant presented a 1.77-fold increase in the EPA/TFA ratio and a 4.05-fold increase in the EPA titer. This is the greatest increase among the strains of *Schizochytrium* sp. obtained by mutagenesis technology. This study lays the foundation for future strain mutagenesis and fermentation optimization for industrial-scale production of EPA, as well as other omega-3 products from *Schizochytrium* strains.

Date availability statement

All data about this study are present in the article and supplementary data.

Acknowledgments

This work was supported by the National Key Research and Development Program of China (No. 2021YFC2100800).

Author contributions

Chao YU designed the research and finished writing the manuscript. Jialin ZHU reviewed and revised the manuscript. Chao YU, Jialin ZHU, Sa ZHAO, Weiwei ZHU, and Min SHU performed the experiments. Shuhuan LU and Xiangyu LI contributed valuable suggestions regarding the optimization of fermentation and the subsequent oil extraction process. Jinyong WU and Mianbin WU supervised the study. Xiangsong CHEN and Jianming YAO conceptualized and supervised the study. All authors have read and approved the final version of the manuscript, and therefore, have full access to all the data in the study and take responsibility for the integrity and security of the data.

Compliance with ethics guidelines

Chao YU, Jialin ZHU, Jinyong WU, Xiangsong CHEN, Shuhuan LU, Xiangyu LI, Sa ZHAO, Weiwei ZHU, Min SHU, Mianbin WU, and Jianming YAO declare that they have no conflicts of interest.

This article does not contain any studies with human or animal subjects performed by any of the authors.

References

Auchterlonie NA, Bescoby GH, 2021. Global market for the long-chain omega-3 fatty acids EPA and DHA and their regulation. *In*: García-Moreno PJ, Jacobsen C, Moltke Sørensen AD, et al. (Eds.), Omega-3 Delivery Systems. Academic Press, London, p.79-106. https://doi.org/10.1016/B978-0-12-821391-9.00014-4

Bazinet RP, Metherel AH, Chen CT, et al., 2020. Brain eicosapentaenoic acid metabolism as a lead for novel therapeutics in major depression. *Brain Behav Immun*, 85:21-28. https://doi.org/10.1016/j.bbi.2019.07.001

Bhatt DL, Steg PG, Miller M, et al., 2019. Effects of icosapent

ethyl on total ischemic events: from REDUCE-IT. *J Am Coll Cardiol*, 73(22):2791-2802. https://doi.org/10.1016/j.jacc.2019.02.032

Calder PC, 2013. *n*-3 Fatty acids, inflammation and immunity: new mechanisms to explain old actions. *Proc Nutr Soc*, 72(3):326-336. https://doi.org/10.1017/S0029665113001031

Chatterjee N, Walker GC, 2017. Mechanisms of DNA damage, repair, and mutagenesis. *Environ Mol Mutagen*, 58(5): 235-263. https://doi.org/10.1002/em.22087

Chen ZL, Yang LH, He SJ, et al., 2023. Development of a green fermentation strategy with resource cycle for the docosahexaenoic acid production by *Schizochytrium* sp. *Bioresour Technol*, 385:129434. https://doi.org/10.1016/j.biortech.2023.129434

Derwenskus F, Weickert S, Lewandowski I, et al., 2020. Economic evaluation of up- and downstream scenarios for the co-production of fucoxanthin and eicosapentaenoic acid with *P. tricornutum* using flat-panel airlift photobioreactors with artificial light. *Algal Res*, 51:102078. https://doi.org/10.1016/j.algal.2020.102078

Doaei S, Gholami S, Rastgoo S, et al., 2021. The effect of omega-3 fatty acid supplementation on clinical and biochemical parameters of critically ill patients with COVID-19: a randomized clinical trial. *J Transl Med*, 19:128. https://doi.org/10.1186/s12967-021-02795-5

Dong W, Zhang YQ, Zhang B, et al., 2013. Rapid prediction of fatty acid composition of vegetable oil by Raman spectroscopy coupled with least squares support vector machines. *J Raman Spectrosc*, 44(12):1739-1745. https://doi.org/10.1002/jrs.4386

Du F, Wang YZ, Xu YS, et al., 2021. Biotechnological production of lipid and terpenoid from Thraustochytrids. *Biotechnol Adv*, 48:107725. https://doi.org/10.1016/j.biotechadv.2021.107725

Golay PA, Moulin J, 2016. Determination of labeled fatty acids content in milk products, infant formula, and adult/pediatric nutritional formula by capillary gas chromatography: collaborative study, final action 2012.13. *J AOAC Int*, 99(1):210-222. https://doi.org/10.5740/jaoacint.15-0140

González-Martín MI, Escuredo O, Hernández-Jiménez M, et al., 2021. Prediction of stable isotopes and fatty acids in subcutaneous fat of Iberian pigs by means of NIR: a comparison between benchtop and portable systems. *Talanta*, 224:121817. https://doi.org/10.1016/j.talanta.2020.121817

Gupta A, Wilkens S, Adcock JL, et al., 2013. Pollen baiting facilitates the isolation of marine Thraustochytrids with potential in omega-3 and biodiesel production. *J Ind Microbiol Biotechnol*, 40(11):1231-1240. https://doi.org/10.1007/s10295-013-1324-0

Hamilton HA, Newton R, Auchterlonie NA, et al., 2020. Systems approach to quantify the global omega-3 fatty acid cycle. *Nat Food*, 1:59-62. https://doi.org/10.1038/s43016-019-0006-0

Jia YL, Geng SS, Du F, et al., 2022. Progress of metabolic engineering for the production of eicosapentaenoic acid. *Crit Rev Biotechnol*, 42(6):838-855. https://doi.org/10.1080/07388551.2021.1971621

Jiang Y, Fan KW, Wong RTY, et al., 2004. Fatty acid composition and squalene content of the marine microalga *Schizochytrium mangrovei*. *J Agric Food Chem*, 52(5):1196-1200. https://doi.org/10.1021/jf035004c

Karunathilaka SR, Choi SH, Mossoba MM, et al., 2019. Rapid classification and quantification of marine oil omega-3 supplements using ATR-FTIR, FT-NIR and chemometrics. *J Food Compos Anal*, 77:9-19. https://doi.org/10.1016/j.jfca.2018.12.009

Khan SU, Lone AN, Khan MS, et al., 2021. Effect of omega-3 fatty acids on cardiovascular outcomes: a systematic review and meta-analysis. *eClinicalMedicine*, 38:100997. https://doi.org/10.1016/j.eclinm.2021.100997

Koláčková P, Růžičková G, Gregor T, et al., 2015. Quick method (FT-NIR) for the determination of oil and major fatty acids content in whole achenes of milk thistle (*Silybum marianum* (L.) Gaertn.). *J Sci Food Agric*, 95(11):2264-2270. https://doi.org/10.1002/jsfa.6945

Kosmopoulos A, Bhatt DL, Meglis G, et al., 2021. A randomized trial of icosapent ethyl in ambulatory patients with COVID-19. *iScience*, 24(9):103040. https://doi.org/10.1016/j.isci.2021.103040

Lamon-Fava S, So J, Mischoulon D, et al., 2021. Dose- and time-dependent increase in circulating anti-inflammatory and pro-resolving lipid mediators following eicosapentaenoic acid supplementation in patients with major depressive disorder and chronic inflammation. *Prostaglandins Leukot Essent Fatty Acids*, 164:102219. https://doi.org/10.1016/j.plefa.2020.102219

Lee TH, Chang JS, Wang HY, 2013. Rapid and in vivo quantification of cellular lipids in *Chlorella vulgaris* using near-infrared Raman spectrometry. *Anal Chem*, 85(4):2155-2160. https://doi.org/10.1021/ac3028118

Ling XP, Guo J, Liu XT, et al., 2015. Impact of carbon and nitrogen feeding strategy on high production of biomass and docosahexaenoic acid (DHA) by *Schizochytrium* sp. LU310. *Bioresour Technol*, 184:139-147. https://doi.org/10.1016/j.biortech.2014.09.130

Liu L, Bai MH, Zhang S, et al., 2021. ARTP mutagenesis of *Schizochytrium* sp. PKU#Mn4 and clethodim-based mutant screening for enhanced docosahexaenoic acid accumulation. *Mar Drugs*, 19(10):564. https://doi.org/10.3390/md19100564

Liu YY, Tian YY, Cai WZ, et al., 2021. DHA/EPA-enriched phosphatidylcholine suppresses tumor growth and metastasis via activating peroxisome proliferator-activated receptor γ in Lewis lung cancer mice. *J Agric Food Chem*, 69(2):676-685. https://doi.org/10.1021/acs.jafc.0c06890

Morabit Y, Hasan MI, Whalley RD, et al., 2021. A review of the gas and liquid phase interactions in low-temperature plasma jets used for biomedical applications. *Eur Phys J D*, 75:32. https://doi.org/10.1140/epjd/s10053-020-00004-4

Ou Y, Li YQ, Feng SS, et al., 2023. Transcriptome analysis reveals an eicosapentaenoic acid accumulation mechanism

in a *Schizochytrium* sp. mutant. *Microbiol Spectr*, 11(3): e0013023.
https://doi.org/10.1128/spectrum.00130-23

Peng ZL, Zhang C, Yan L, et al., 2020. EPA is more effective than DHA to improve depression-like behavior, glia cell dysfunction and hippcampal apoptosis signaling in a chronic stress-induced rat model of depression. *Int J Mol Sci*, 21(5):1769.
https://doi.org/10.3390/ijms21051769

Preston Mason R, 2019. New insights into mechanisms of action for omega-3 fatty acids in atherothrombotic cardiovascular disease. *Curr Atheroscler Rep*, 21:2.
https://doi.org/10.1007/s11883-019-0762-1

Ratledge C, Hopkins S, 2006. Applications and safety of microbial oils in food. *In*: Gunstone FD (Ed.), Modifying Lipids for Use in Food. Woodhead Publishing, Cambridge, p.567-586.
https://doi.org/10.1533/9781845691684.3.567

Reis MG, Agnew M, Jacob N, et al., 2022. Comparative evaluation of miniaturized and conventional NIR spectrophotometer for estimation of fatty acids in cheeses. *Spectrochim Acta Part A Mol Biomol Spectrosc*, 279:121433.
https://doi.org/10.1016/j.saa.2022.121433

Ren LJ, Feng Y, Li J, et al., 2013. Impact of phosphate concentration on docosahexaenoic acid production and related enzyme activities in fermentation of *Schizochytrium* sp. *Bioprocess Biosyst Eng*, 36(9):1177-1183.
https://doi.org/10.1007/s00449-012-0844-8

Rosenberg SM, 2013. Reverse mutation. *In*: Maloy S, Hughes K (Eds.), Brenner's Encyclopedia of Genetics, 2nd Ed. Academic Press, Amsterdam, p.220-221.
https://doi.org/10.1016/B978-0-12-374984-0.01325-5

Shen J, Zhang H, Xu ZM, et al., 2019. Preferential production of reactive species and bactericidal efficacy of gas-liquid plasma discharge. *Chem Eng J*, 362:402-412.
https://doi.org/10.1016/j.cej.2019.01.018

Shene C, Paredes P, Vergara D, et al., 2020. Antarctic Thraustochytrids: producers of long-chain omega-3 polyunsaturated fatty acids. *MicrobiologyOpen*, 9:e00950.
https://doi.org/10.1002/mbo3.950

Sun XM, Ren LJ, Bi ZQ, et al., 2018a. Adaptive evolution of microalgae *Schizochytrium* sp. under high salinity stress to alleviate oxidative damage and improve lipid biosynthesis. *Bioresour Technol*, 267:438-444.
https://doi.org/10.1016/j.biortech.2018.07.079

Sun XM, Ren LJ, Bi ZQ, et al., 2018b. Development of a cooperative two-factor adaptive-evolution method to enhance lipid production and prevent lipid peroxidation in *Schizochytrium* sp. *Biotechnol Biofuels*, 11:65.
https://doi.org/10.1186/s13068-018-1065-4

Tsegay G, Ammare Y, Mesfin S, 2023. Development of non-destructive NIRS models to predict oil and major fatty acid contents of Ethiopian sesame. *J Food Compos Anal*, 115:104908.
https://doi.org/10.1016/j.jfca.2022.104908

Wang QY, Li ZG, Ma ZH, et al., 2014. Real time monitoring of multiple components in wine fermentation using an online auto-calibration Raman spectroscopy. *Sens Actuators B Chem*, 202:426-432.
https://doi.org/10.1016/j.snb.2014.05.109

Wang S, Wan WJ, Wang ZJ, et al., 2021. A two-stage adaptive laboratory evolution strategy to enhance docosahexaenoic acid synthesis in oleaginous thraustochytrid. *Front Nutr*, 8:795491.
https://doi.org/10.3389/fnut.2021.795491

Wei XY, Wang YZ, Liu XN, et al., 2023. Metabolic analysis of *Schizochytrium* sp. mutants with high EPA content achieved with ARTP mutagenesis screening. *Bioprocess Biosyst Eng*, 46(6):893-901.
https://doi.org/10.1007/s00449-023-02874-5

Xiao BP, Li YY, Lin YQ, et al., 2022. Eicosapentaenoic acid (EPA) exhibits antioxidant activity via mitochondrial modulation. *Food Chem*, 373:131389.
https://doi.org/10.1016/j.foodchem.2021.131389

Yin FW, Zhang YT, Jiang JY, et al., 2019. Efficient docosahexaenoic acid production by *Schizochytrium* sp. via a two-phase pH control strategy using ammonia and citric acid as pH regulators. *Process Biochem*, 77:1-7.
https://doi.org/10.1016/j.procbio.2018.11.013

Yin HW, Liu YY, Yue H, et al., 2022. DHA- and EPA-enriched phosphatidylcholine suppress human lung carcinoma 95D cells metastasis via activating the peroxisome proliferator-activated receptor γ. *Nutrients*, 14(21):4675.
https://doi.org/10.3390/nu14214675

Yu HW, Liu HZ, Wang Q, et al., 2020. Evaluation of portable and benchtop NIR for classification of high oleic acid peanuts and fatty acid quantitation. *LWT*, 128:109398.
https://doi.org/10.1016/j.lwt.2020.109398

Yue XH, Chen WC, Wang ZM, et al., 2019. Lipid distribution pattern and transcriptomic insights revealed the potential mechanism of docosahexaenoic acid traffics in *Schizochytrium* sp. A-2. *J Agric Food Chem*, 67(34):9683-9693.
https://doi.org/10.1021/acs.jafc.9b03536

Zeng L, Bi YQ, Guo PF, et al., 2021. Metabolic analysis of *Schizochytrium* mutants with high DHA content achieved with ARTP mutagenesis combined with iodoacetic acid and dehydroepiandrosterone screening. *Front Bioeng Biotechnol*, 9:738052.
https://doi.org/10.3389/fbioe.2021.738052

Zeng WZ, Guo LK, Xu S, et al., 2020. High-throughput screening technology in industrial biotechnology. *Trends Biotechnol*, 38(8):888-906.
https://doi.org/10.1016/j.tibtech.2020.01.001

Zhu YF, Huang XY, Han T, et al., 2025. Improvement of neutral protease activity of *Bacillus amyloliquefaciens* LX-6 by combined ribosome engineering and medium optimization. *J Zhejiang Univ-Sci B (Biomed & Biotechnol)*, 26(8): 805-812.
https://doi.org/10.1631/jzus.B2400477

Supplementary information

Figs. S1–S5; Table S1